J. Phys.: Condens. Matter 7 (1995) 2783–2799. Printed in the UK

Relativistic band structure of ternary II–VI semiconductor alloys containing Cd, Zn, Se and Te

H C Poon†, Z C Feng†, Y P Feng† and M F Li ‡

† Department of Physics, National University of Singapore, Kent Ridge, Singapore 0511
‡ Centre for Optoelectronics, Department of Electrical Engineering, National University of Singapore, Kent Ridge, Singapore 0511

Received 11 October 1994, in final form 28 November 1994

Abstract. The relativistic band structure and band-gap bowing factors of ternary II–VI semiconductor alloys containing Cd, Zn, Se and Te are calculated by the *ab initio* self-consistent pseudopotential method with spin–orbit correction. The disorder in these alloys is modelled by the virtual crystal approximation (VCA). The numerical results thus obtained are compared with experimental data from photoluminescence spectroscopy. The experimental band-gap bowings for this family of alloys are always concave upwards. However, $CdSe_xTe_{1-x}$ and $ZnSe_xTe_{1-x}$ in general show much larger bowing factors than $Cd_{1-x}Zn_xSe$ and $Cd_{1-x}Zn_xTe$. The former two alloys show a minimum in the band gap versus composition curve near $x = 0.35$ while the latter two have it at $x = 0$. Most of these qualitative trends are well explained by VCA. However, in order to explain the large bowing in the first two alloys, some kind of local order has to be incorporated in the calculation. It was found that a local cluster with AuCu-I-like structure, when relaxed, has quite a significant contribution to the bowing factors. The splittings in the band structure due to both spin–orbit and structural relaxation effects are also discussed.

1. Introduction

Different methods have been applied in the calculation of the band structure of II–VI semiconductor alloys. These include methods based on the dielectric two-band model [1], semiempirical tight-binding method [2], semiempirical pseudopotential method [3] and self-consistent method using local density-functional approximation (LDA) [4]. Traditionally, because of its simplicity, the virtual crystal approximation (VCA) is preferred for the treatment of chemical disorder in semiconductor alloys. In VCA, the potential of each atom in the alloy is replaced by a weighted average of the potentials of its components. It does lead to qualitative explanation of most of the features in the bowing factors of semiconductor alloys. Unfortunately, with few exceptions, most of these methods are not free of adjustable parameters. Based on the self-consistent calculation of the band structure of II–VI alloys, it has been found [4] that a local relaxation effects plays a significant role in causing the bowing of the band-structure energy versus composition x for certain semiconductor alloys. For such systems, VCA vastly underestimates the bowing of the band structure.

The purpose of the present work is to present a systematic study of the band structure and the band-gap bowing factors of the $Cd_{1-x}Zn_xSe_yTe_{1-y}$ family with either $x = 0$, $x = 1$, $y = 0$ or $y = 1$ using both the VCA and the locally ordered cluster approach. The computational method used is the *ab initio* self-consistent pseudopotential method with spin–orbit correction. Comparison is made with experimental data from photoluminescence

0953-8984/95/142783+17$19.50

(PL) spectroscopy. Such comparison enables us to assess the importance of local order in these compounds. Owing to the existence of local order and possibly atomic relaxation, the band structure in the alloys is distinctly different from that by VCA. The splittings due to both structural and spin–orbit effects is discussed. In section 2 a brief description of the method of calculation is presented. Section 3 is a summary of the experimental procedures. Comparison of the calculation with experimental data is found in section 4. Section 5 is the conclusion.

2. Method of calculation

The relativistic norm-conserving pseudopotentials of the ion cores of Cd, Zn, Se and Te are constructed using a method due to Kleinman [5] and Bachelet *et al* [6]. It can be written as

$$V_{\rm ps}^{\rm ion}(r) = \sum_l |l\rangle [V_l^{\rm ion}(r) + V_l^{\rm so}(r) \boldsymbol{L}\cdot\boldsymbol{S}] \langle l| \tag{1}$$

where

$$V_l^{\rm ion}(r) = [1/(2l+1)][(l+1)V_{l+1/2}^{\rm ion}(r) + lV_{l-1/2}^{\rm ion}(r)] \tag{2}$$

is the average pseudopotential and

$$V_l^{\rm so}(r) = [2/(2l+1)](V_{l+1/2}^{\rm ion}(r) - V_{l-1/2}^{\rm ion}(r)) \tag{3}$$

is the spin–orbit correction. $V_{l+1/2}^{\rm ion}(r)$ and $V_{l-1/2}^{\rm ion}(r)$ are the relativistic norm-conserving ion-core pseudopotentials constructed from all-electron self-consistent atomic potential, which is in turn obtained by solving the Dirac equation. The summation over angular momenta is up to $l = 2$.

Consider a ternary semiconductor alloy of the form $A_{1-x}B_xC$ containing any three of the four elements. Under VCA, the pseudopotential at $\boldsymbol{r}$ due to all the ion cores is given by

$$V_{\rm ps}(\boldsymbol{r}) = \sum_{i,j} [(1-x)V^{\rm A}(\boldsymbol{r}-\boldsymbol{R}_i) + xV^{\rm B}(\boldsymbol{r}-\boldsymbol{R}_i) + V^{\rm C}(\boldsymbol{r}-\boldsymbol{R}_j)]. \tag{4}$$

The sum is over the positions of the two sublattices i and j. Either A, B are the column II and C the column VI elements, or A, B are the column VI and C the column II elements. There are four combinations in total.

Experimental evidence indicates that locally ordered structures exist in certain III–V and II–VI semiconductor alloys [7–13]. In order to simulate the local order effect, we have considered local clusters of the form ABC_2 (see figure 1). Owing to the very large spin–orbit splittings that the valence states of II–VI compounds possess, we have included spin–orbit correction in our calculation. For simplicity, the 3d electrons in Zn and Se, together with core electrons having lower energy, are frozen in the ion core and not considered as valence electrons. Similarly, the 4d electrons in Cd and Te are frozen. Previous work [14] with 3d and 4d included as valence electrons leads to a reduction of band gaps in II–VI semiconductors. If we assume that the reduction is linear in alloy composition, the bowing factor will not be seriously affected. This assumption seems to be justified when we compare the bowing factor calculated here with previous values with 3d and 4d included

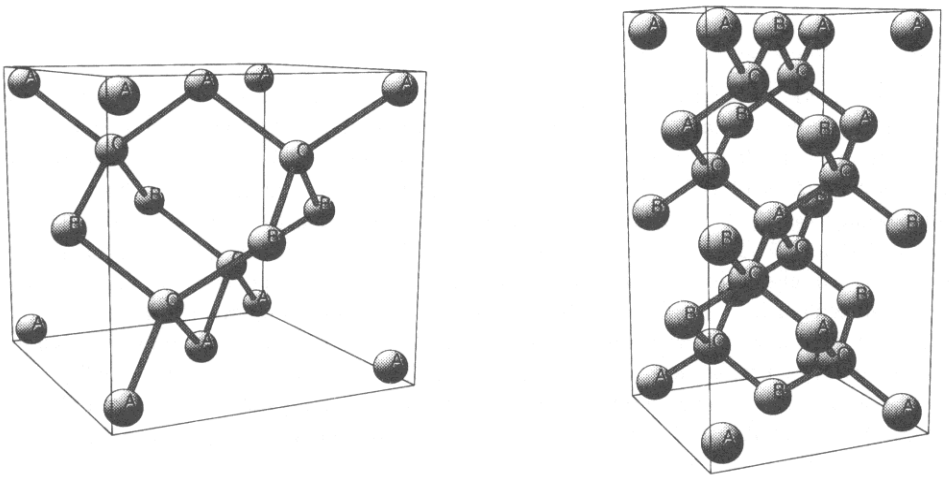

(a) (b)

Figure 1. Local clusters of form ABC_2 in II–VI zincblende semiconductor alloys: (*a*) AuCu-I-like structure; (*b*) chalcopyrite structure.

for the case of $ZnSe_xTe_{1-x}$. As will be seen, even in the absence of 3d and 4d in the valence states, the calculated spin–orbit splittings agree quite well with experiment. The reason is that the effect of spin–orbit mixing of relativistic d core and valence states has been included automatically in the formalism for the atomic pseudo-wavefunctions. Further details can be found in [15]. Consequently, the pseudopotential seen by all the valence electrons is weak and only a small plane-wave basis is needed to achieve convergence.

The Hamiltonian of the crystal can be written as

$$H = p^2/2m + V_{ps} + V_H + V_{xc} \tag{5}$$

where $p^2/2m$ is the kinetic energy of a valence electron, and V_H and V_{xc} are the Coulomb and exchange–correlation potentials acting on the valence electrons. The Ceperly and Alder interpolation formula for exchange–correlation energy [16] is used in both the atomic and crystal calculation. Matrix elements of the various terms of the Hamiltonian and spin–orbit correction in the plane-wave basis can be found in [7] and [15]. In the present self-consistent calculation, the wavefunction is expanded in a basis set of plane waves corresponding to a cut-off energy of 16 Ryd. Ten special k-points are taken. Typically, for the family of alloys considered here, less than 10 iterations are required to achieve a convergence of 0.0001 Ryd in potential.

LDA is known to give incorrect band gaps in semiconductors and insulators. In order to describe the true single-particle excitation energy, a dynamical self-energy correction needs to be included [17]. Such a calculation is computationally quite demanding, especially for those large unit cells adopted here. Since we are more interested in the band-gap bowing factor, the band gaps for the endpoint compounds are taken from experiments and the LDA band gaps for intermediate compositions are calculated. It is assumed that the self-energy correction is proportional to composition, and the bowing factor is not expected to be seriously affected.

3. Experiment

3.1. Sample preparation

In the present work, experimental samples of CdZnTe and CdSeTe bulk alloys were prepared using the Bridgman technique. They were prepared by reacting the 99.9999% pure elemental constituents at $\sim$ 1150 °C in evacuated, sealed quartz tubes, and regrown by directional solidification at rates of 0.8–1.2 mm h^{-1} in a Bridgman–Stockbarger-type furnace. The resultant boules were cut into slices 1–2 mm thick, perpendicular to the growth axis. These were annealed at 600 °C in a Cd atmosphere for CdZnTe, or at 650 °C in a Se atmosphere for CdSeTe, respectively, to improve the crystalline perfection. Consequently they were lapped, polished and etched in a bromine–methanol solution. The alloy compositions were set by the ratio of constituents before growth, and confirmed by x-ray diffraction and transmission measurements after preparation. For CdZnTe, x ranges over all x; and for CdSeTe, x is between 0 and 0.35. These samples are found to be single-crystal with the zincblende structure. More details of the preparation of these single-crystal samples can be found elsewhere [18, 19].

3.2. Room-temperature photoluminescence measurement

The room-temperature (RT) PL measurements were performed using a new Renishaw model 2000 Raman and PL spectrometer with a single grating, notch filter, microprobe capability and CCD (charge-coupled device) detection. The excitation used was He–Ne 633 nm with approximately 1 mW at the sample over a spot of about 1 mm diameter. In earlier measurements, using a standard double spectrometer/photomultiplier/photon counting system, or a triple spectrometer/Si array optical multichannel analyser detection system, we obtained PL spectra of these same samples below 150 K, but could not obtain PL spectra at room temperature. By the help of this sensitive and efficient Renishaw Raman/PL microscope, nice RT PL spectra with high signal-to-noise ratio for all the CdZnTe and CdSeTe compounds were obtained, which can be seen from the next section.

3.3. Photoluminescence spectra of CdZnTe and CdSeTe

Figure 2 exhibits the RT PL spectra of $Cd_{1-x}Zn_{1-x}Te$, with $x = 0$ (i.e. pure CdTe), 0.01, 0.10, 0.30 and 0.50. It shows that the PL band shifts up in energy as x increases from 0 to 0.50, indicating an increase in the energy band gap.

Figure 3 displays RT PL spectra of $CdSe_xTe_{1-x}$, with $x = 0.05$, 0.15, 0.25 and 0.35. The spectra of $x = 0$ or pure CdTe is also shown here for comparison. In the reverse of the above CdZnTe case, the PL band shifts down in energy as x increases from 0 to 0.35, indicating a decrease in the energy band gap for CdSeTe as $x < 0.36$ [20].

We also made absorption measurements on these samples (not shown here) and the same result was obtained. More work on PL of $CdSe_xTe_{1-x}$ and $Cd_{1-x}Zn_{1-x}Te$ with more different compositions and their variations with temperature and time are in process and will be published later.

4. Results and discussions

4.1. Virtual crystal approximation (VCA)

By employing VCA, the self-consistent band structures of ternary alloys containing Cd, Zn, Se and Te are calculated. The lattice constants of CdSe, CdTe, ZnSe, and ZnTe are taken

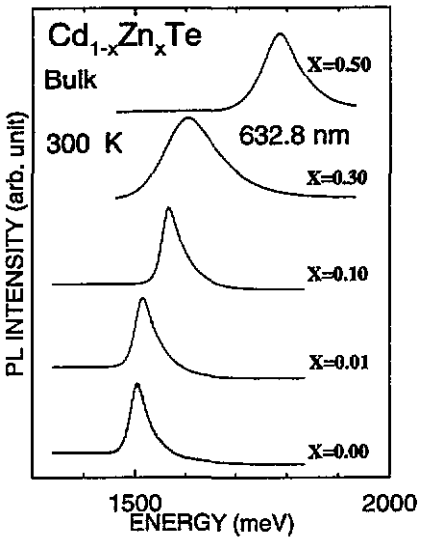

Figure 2. Room-temperature photoluminescence of bulk $Cd_{1-x}Zn_xTe$ with $x = 0$, 0.01, 0.10, 0.30 and 0.50 respectively.

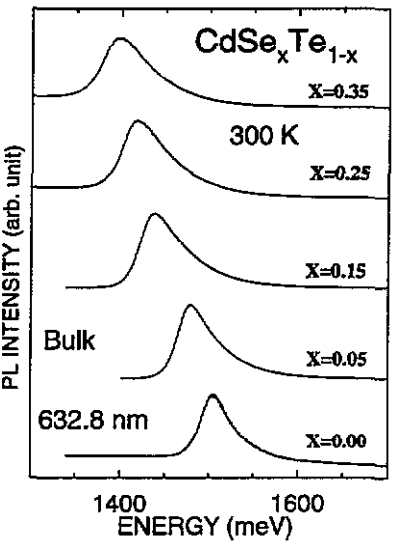

Figure 3. Room-temperature photoluminescence of bulk $CdSe_xTe_{1-x}$ with $x = 0$, 0.05, 0.15, 0.25 and 0.35 respectively.

from experimental measurements. They are 6.050, 6.480, 5.668 and 6.089 Å, respectively. There are two possible crystal structures for these compounds—the zincblende and the wurtzite structures. Previous work [21] has shown that the band structures of the two different crystal structures are essentially the same, except for small shifts of energy levels. For convenience, the crystal structures of all these semiconductor compounds are assumed to have the cubic zincblende structure, although the common form of CdSe is known to have the wurtzite structure. By Vegard's rule, the variation of lattice constant with composition is assumed to be linear. Some typical band structures at compositions $x = 0$ and 1 are shown in figure 4. The band structures for $x = 0.5$ are shown in figure 5. Both the band structures with and without spin–orbit splitting are shown in the figures. The band gaps are direct for all the cases considered. From this we find the calculated band gap as a function of composition. These are shown in figure 6. In the figure, we have used the experimental band gaps at $x = 0$ and $x = 1$. We also assume that the error in taking the LDA at $x = 0.5$ is the average of the errors at $x = 0$ and $x = 1$. The corresponding experimental results for $Cd_{1-x}Zn_{1-x}Te$ and $CdSe_xTe_{1-x}$ alloys from photoluminescence and absorption spectroscopies are shown in figure 7. The calculated and experimental band gaps for $x = 0$, 0.5 and 1 are compared in table 1. Assuming that the band gap versus composition curve is quadratic, the bowing factor is given by the relation

$$E_g(x) = (1-x)E_0 + xE_1 - bx(1-x). \tag{6}$$

The bowing factor can be explicitly expressed in terms of the band gaps at three different x values as follows:

$$b = 2(E_0 + E_1) - 4E_{1/2} \tag{7}$$

where E_0 and E_1 are the band gaps for $x = 0$ and $x = 1$ respectively and $E_{1/2}$ is that for $x = 1/2$. The spin–orbit bowing factor is similarly defined with $E_g(x)$ replaced by $\Delta(x)$, the spin–orbit splitting at the top of the valence band at Γ.

Table 1. The calculated band gaps of ternary semiconductor alloys containing Cd, Zn, Se and Te with $x = 0$, 0.5 and 1 by using VCA. Experimental values are from the present work and [22].

	Band gap (eV)	
	Calculated	Experiment
CdSe	0.91	1.78
CdTe	0.82	1.60
ZnSe	1.41	2.82
ZnTe	1.22	2.39
$CdSe_{0.5}Te_{0.5}$	0.79	1.48
$ZnSe_{0.5}Te_{0.5}$	1.26	2.23
$Cd_{0.5}Zn_{0.5}Se$	1.11	2.21
$Cd_{0.5}Zn_{0.5}Te$	1.01	1.92

The calculated and experimental band-gap bowing factors for the alloys are shown in table 2. For $Cd_{1-x}Zn_xSe$, there is a structural phase transition from wurtzite to zincblende structure in the composition region $0.5 < x < 0.7$ [25]. The difference between the experimental band-gap values of ZnSe-wurtzite and ZnSe-zincblende structures is about 0.06 eV [26] while the experimental values of the bowing factors are about the same for the two different structures. They are both about 0.35 eV [24].

One may question whether Vegard's rule really holds for the family of compounds considered here. Therefore, we have also performed calculations in which the lattice constants are found by the minimization of the total energy. Typically the lattice constants found in this way differ by less than a few per cent from the experimental values at $x = 0$ and $x = 1$. The curves for the lattice constant as a function of composition for $CdSe_xTe_{1-x}$ and $Cd_{1-x}Zn_xSe$ are shown in figure 8. It is seen that Vegard's rule is not strictly obeyed. The bowing is especially significant for $Cd_{1-x}Zn_xSe$. In spite of this, no qualitative change is observed in the relation between band gap and composition when these lattice constants are used in place of those by Vegard's rule.

It is well known that calculation using LDA underestimates the band-gap values of III–V and II–VI semiconductors. From table 1, it is seen that the calculated values are almost two times less than the experimental values at $x = 0$ and $x = 1$ for all the cases considered here. Assuming that the error in the band gap using LDA is a linear function of intermediate composition, the bowing factor will remain roughly the same. If we compare the calculated bowing factors with experimental ones (table 2), the agreement is less than satisfactory. It is seen that VCA vastly underestimates the band-gap bowing factors of $CdSe_xTe_{1-x}$ and $ZnSe_xTe_{1-x}$. Experiments done at different temperatures in certain cases show quite some variation of the bowing factor with temperature. No temperature effect has been included in the above calculations. The calculated values should be compared with data taken at low temperature whenever possible. Another reason may be due to the VCA itself. The role played by the local order effect will be discussed in the next section.

However, it is worth noting that several important features in the experimental data are reproduced by the calculation. First of all, the calculated bowing is always concave upwards as in experiment. Secondly, it is noted that, for the case of $CdSe_xTe_{1-x}$, the calculated curve exhibits a minimum at $x = 0.35$ as was found in experiment. On the other hand, for $ZnSe_xTe_{1-x}$ the minimum found in the calculation is close to $x = 0$ while the experimental value is $x = 0.35$. The experimental band gaps of $CdSe_xTe_{1-x}$ and $ZnSe_xTe_{1-x}$ show much larger bowing factors than $Cd_{1-x}Zn_xSe$ and $Cd_{1-x}Zn_xTe$. The calculated values for the former two cases are much smaller than the experimental values. It indicates that VCA

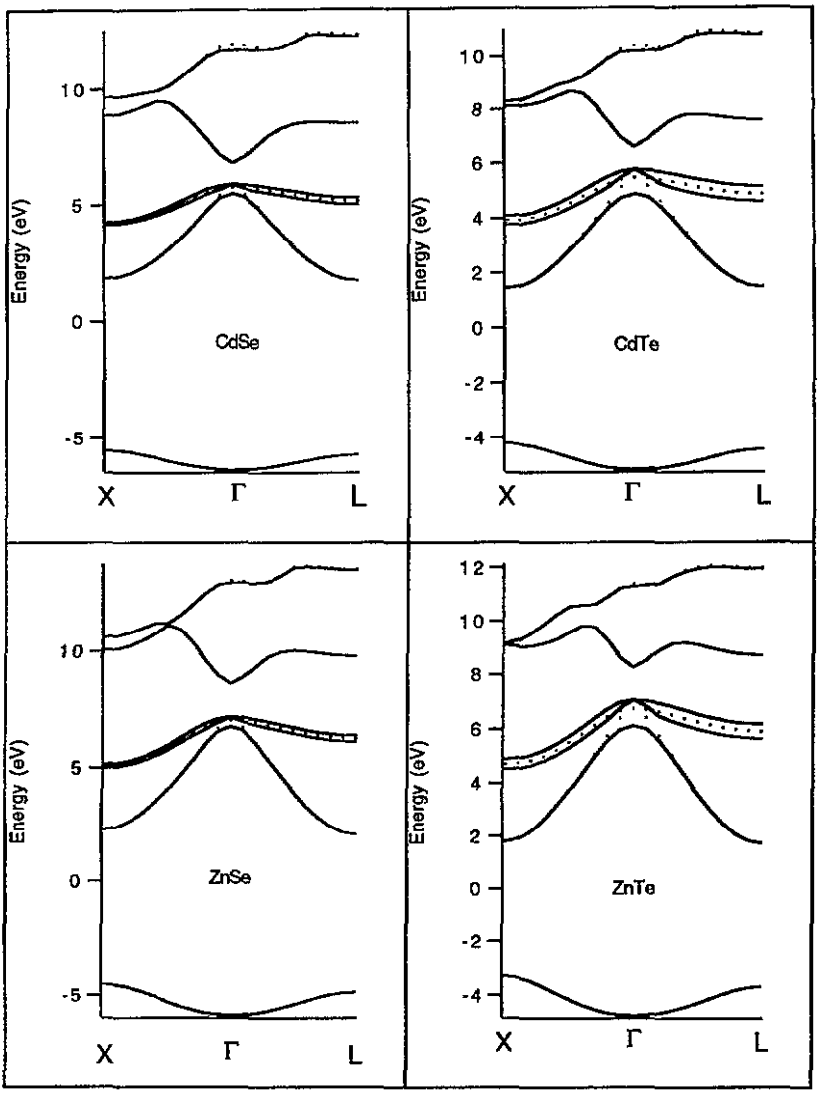

Figure 4. Calculated band structure along ΓX and ΓL for ternary II–VI semiconductor alloys containing Cd, Zn, Se and Te at $x = 0$ and 1 by using VCA. (Full and dotted curves represent band structure with and without spin–orbit correction respectively.)

is no longer valid and some kind of local order may exist in these alloys.

Finally the spin–orbit splittings at the top of the valence band at the Γ point for different compositions are shown in table 3. The spin–orbit bowing factors are shown in table 4. The bowings are negative, i.e. concave downwards, for all cases. The calculation shows negligible bowing in the spin–orbit splittings of $Cd_{1-x}Zn_xSe$ and $Cd_{1-x}Zn_xTe$, while the contribution of spin–orbit effect to the bowing is about −0.32 eV for both $CdSe_xTe_{1-x}$ and $ZnSe_xTe_{1-x}$. It is seen from table 3 that, for $x = 0$ and $x = 1$, the first-principles results agree quite well with experimental data and previous theoretical calculation by the semiempirical pseudopotential method [21, 27–29].

As mentioned above, VCA has completely ignored the local order effect. Its contribution

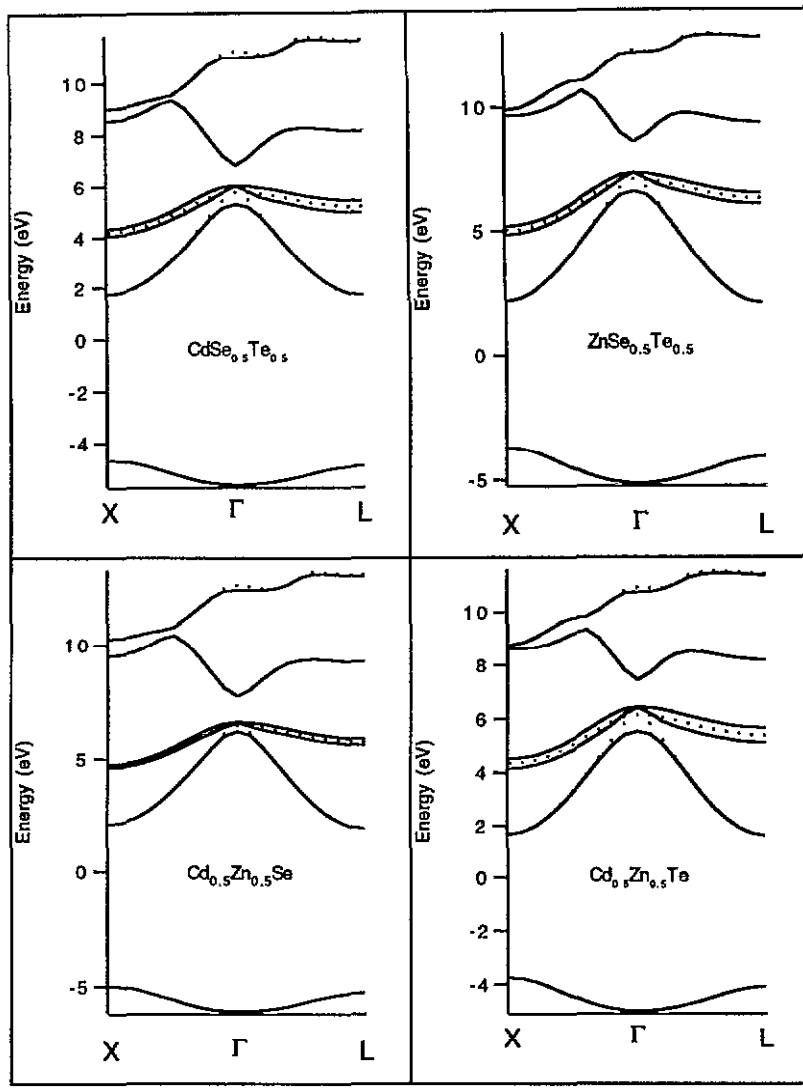

Figure 5. Calculated band structure along ΓX and ΓL for ternary II–VI semiconductor alloys containing Cd, Zn, Se and Te at $x = 0.5$ by using VCA. (Full and dotted curves represent band structure with and without spin–orbit correction respectively.)

to the bowing factors of the compounds considered here will be considered in the next section.

4.2. Bowing factor

Previous work [4] on ternary alloys has shown that, for certain cases, local order with relaxation accounts for most of the bowing effect in the band structure. The local order effect is simulated here by an AuCu-I-like structure. This is the 50%–50% structure with the smallest unit cell. A more complicated 50%–50% structure (chalcopyrite) is also possible. According to the Landau–Lifshitz theory of order-disorder transitions [30], these are the only major structures in the alloy at $x = 0.5$. The two structures are shown in figure 1.

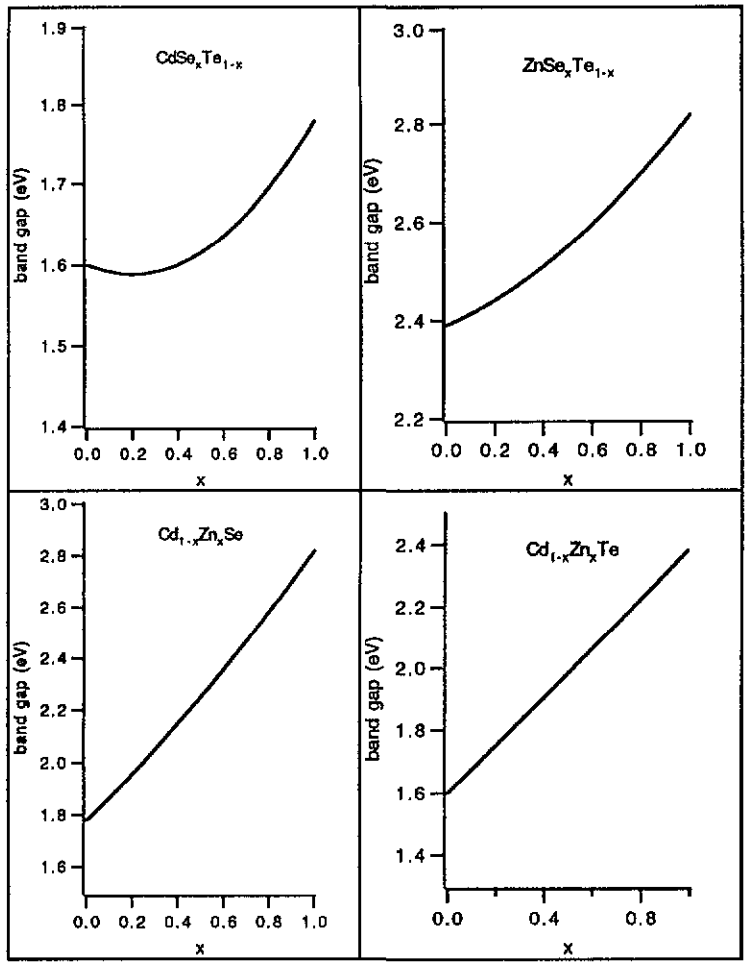

Figure 6. Calculated band gap versus composition x for II–VI ternary alloys containing Cd, Zn, Se and Te by using VCA. The calculated curve has been adjusted by an amount proportional to x so that the values at the two endpoint coincide with experimental values.

We first consider the AuCu-I-like structure. The calculation proceeds as before, except now we have a periodic structure with four atoms/cell instead of two atoms/cell in VCA. The corresponding band-gap bowing factors for various ternary II–VI alloys are shown in table 5. For comparison, the values by VCA are also shown. It was suggested [4] that the AuCu-I-like cluster is the dominant species found in $ZnSe_{0.5}Te_{0.5}$. By total energy minimization, it was found that the optimal structure in the alloy is close to one in which the Zn atom moves in such a way that Zn–Se as well as Zn–Te bond lengths equal those of pure ZnSe and ZnTe respectively. We expect that the same kind of relaxation will happen in $CdSe_{0.5}Te_{0.5}$. Referring to figure 1, if we take A, B and C to be Se, Te and Cd atoms respectively, then it corresponds to the downward relaxation of the two lower Cd atoms and also the upward relaxation of the upper two Cd atoms. We find that, for $CdSe_{0.5}Te_{0.5}$, complete relaxation of Cd would lead to a band-gap bowing factor that is too large as compared with experiment. Therefore we have performed a total energy minimization to search for the optimal relaxation parameter. Figure 9 shows the total energy per unit cell

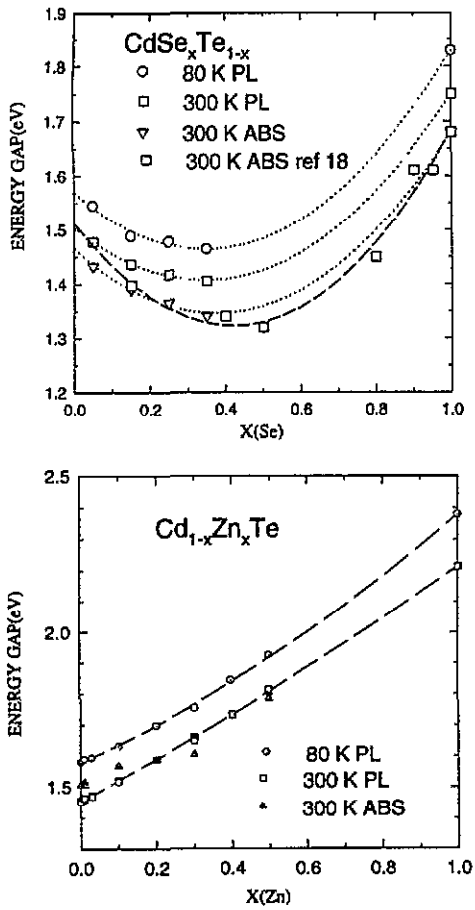

Figure 7. Experimental band gap versus composition x for $CdSe_xTe_{1-x}$ and $Cd_{1-x}Zn_xTe$ at 80 and 300 K.

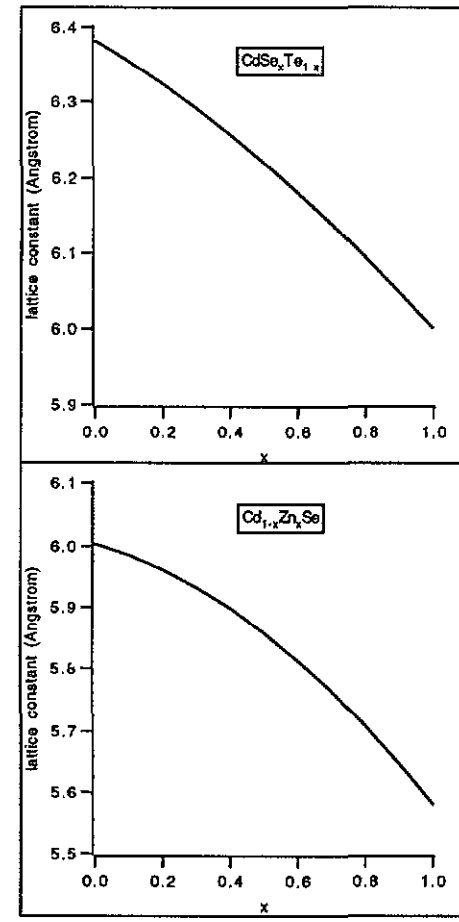

Figure 8. Calculated lattice constant versus composition x for $CdSe_xTe_{1-x}$ and $Cd_{1-x}Zn_xSe$ obtained by total energy minimization.

versus vertical relaxation of Cd (refer to figure 1). In this figure, 0% relaxation means that the Cd–Se and Cd–Te bond lengths in the alloy are the same and equal to the average of Cd–Se and Cd–Te bond lengths in the respective pure semiconductor compounds; 100% relaxation means that the corresponding bond lengths in the alloy retain their values in the pure semiconductor compounds. Complete relaxation in the alloy corresponds to the case where the bond lengths of Cd–Se and Cd–Te are 2.6197 and 2.8059 Å respectively, while the average bond length in the alloy is 2.7128 Å. From figure 9, we find that the relaxation in $CdSe_{0.5}Te_{0.5}$ is about 67%. For the remaining two common-anion alloys, we have assumed complete relaxation (100%), since the band gap depends only weakly on the relaxation. It is interesting to note that previous experiment [7] by x-ray absorption fine structure (EXAFS) on the alloy $Ga_{1-x}In_xAs$ has found that the relaxation of the Ga–As and In–As bonds are about 75%.

Allowing for this kind of relaxation in our local cluster, the new band-gap bowing factors are added to table 5. It is seen that the relaxation significantly lowers the band-gap values of common-cation alloys like $CdSe_xTe_{1-x}$ and $ZnSe_xTe_{1-x}$. On the other hand, for

Table 2. Comparison of band-gap bowing factors from experiment and calculation using VCA for ternary semiconductor alloys containing Cd, Zn, Se and Te.

	b_g (eV)	
	VCA calculation	Experiment
$CdSe_xTe_{1-x}$	0.30	0.90[a]
		0.94[b]
$ZnSe_xTe_{1-x}$	0.22	1.507[c]
		1.621[d]
$Cd_{1-x}Zn_xSe$	0.20	0.35[e]
$Cd_{1-x}Zn_xTe$	0.02	0.25[f]
		0.11[g]

[a] This work (80 K).
[b] [20] (300 K).
[c] [23] (4 K).
[d] [23] (300 K).
[e] [24] (4.2 K, 77 K).
[f] This work (80 K).
[g] This work (300 K).

Table 3. Comparison of the spin–orbit splittings at the top of the valence band from experiment and calculation by VCA for ternary semiconductors containing Cd, Zn, Se and Te with $x = 0$, 0.5 and 1. EPM means values obtained by semiempirical pseudopotential calculation.

	$\Delta(x)$ (eV)		
	Present calculation	Experiment	EPM
CdSe	0.41	0.42[a]	
CdTe	0.91	0.95[b]	0.89[d]
ZnSe	0.42	0.43[a]	0.45[d]
ZnTe	0.92	0.91[c]	
$CdSe_{0.5}Te_{0.5}$	0.74		
$ZnSe_{0.5}Te_{0.5}$	0.75		
$Cd_{0.5}Zn_{0.5}Se$	0.43		
$Cd_{0.5}Zn_{0.5}Te$	0.92		

[a] [27].
[b] [28].
[c] [29].
[d] [21].

Table 4. Calculated spin–orbit bowing factor at the top of the valence band for ternary semiconductors containing Cd, Zn, Se and Te by using VCA.

	b_{so} (eV)
$CdSe_xTe_{1-x}$	−0.32
$ZnSe_xTe_{1-x}$	−0.32
$Cd_{1-x}Zn_xSe$	−0.06
$Cd_{1-x}Zn_xTe$	−0.02

common-anion alloys like $Cd_{1-x}Zn_xSe$ and $Cd_{1-x}Zn_xTe$, the effect is relatively small. It offers an explanation for our experimental observation that common-cation alloys have a much larger bowing that common-anion alloys. The band gap as a function of composition x

Table 5. Comparison of band-gap bowing factors from experiment and calculation using an AuCu-I-like cluster with relaxation for ternary semiconductor alloys containing Cd, Zn, Se and Te. For comparison, the VCA values are also shown. The values in parentheses are from [4].

	b_g (eV)			
	Cluster calculation with relaxation	Cluster calculation without relaxation	VCA calculation	Experiment
$CdSe_xTe_{1-x}$	1.14	0.06	0.30	0.90[a]
				0.94[b]
$ZnSe_xTe_{1-x}$	1.82	0.26	0.22	1.507[c]
	(1.96)			1.621[d]
$Cd_xZn_{1-x}Se$	0.52	0.44	0.20	0.35[e]
$Cd_{1-x}Zn_xTe$	0.48	0.44	0.02	0.25[f]
	(0.35)			0.11[g]

[a] This work (80 K).
[b] [20] (300 K).
[c] [23] (4 K).
[d] [23] (300 K).
[e] [24] (4.2 K, 77 K).
[f] This work (80 K).
[g] This work (300 K).

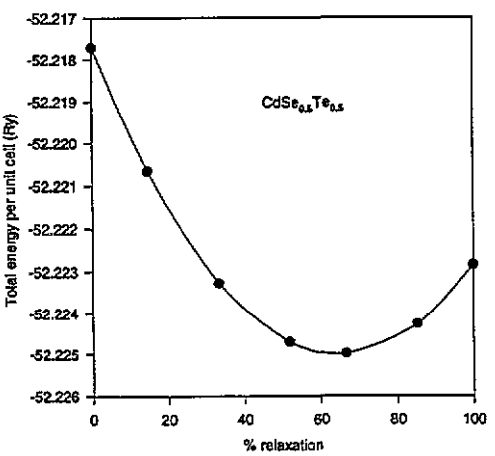

Figure 9. Total energy per unit cell versus percentage relaxation of Cd atom in local cluster of $CdSe_{0.5}Te_{0.5}$.

is shown in figure 10. The agreement with experiment is dramatically improved, especially for $ZnSe_xTe_{1-x}$, for which we know that the experimental minimum is located at $x = 0.35$ [23]. The magnitudes of bowing also agree reasonably well with experiment, indicating that the type of local cluster considered here is indeed the dominant species in the family of alloys containing Cd, Zn, Se and Te.

Since the computation on chalcopyrite structure consisting of eight atoms per unit cell is quite demanding, we have only performed calculation on $CdSe_xTe_{1-x}$, which is the alloy of most interest here. It was found that the bowing factor is quite small (about 0.06 eV).

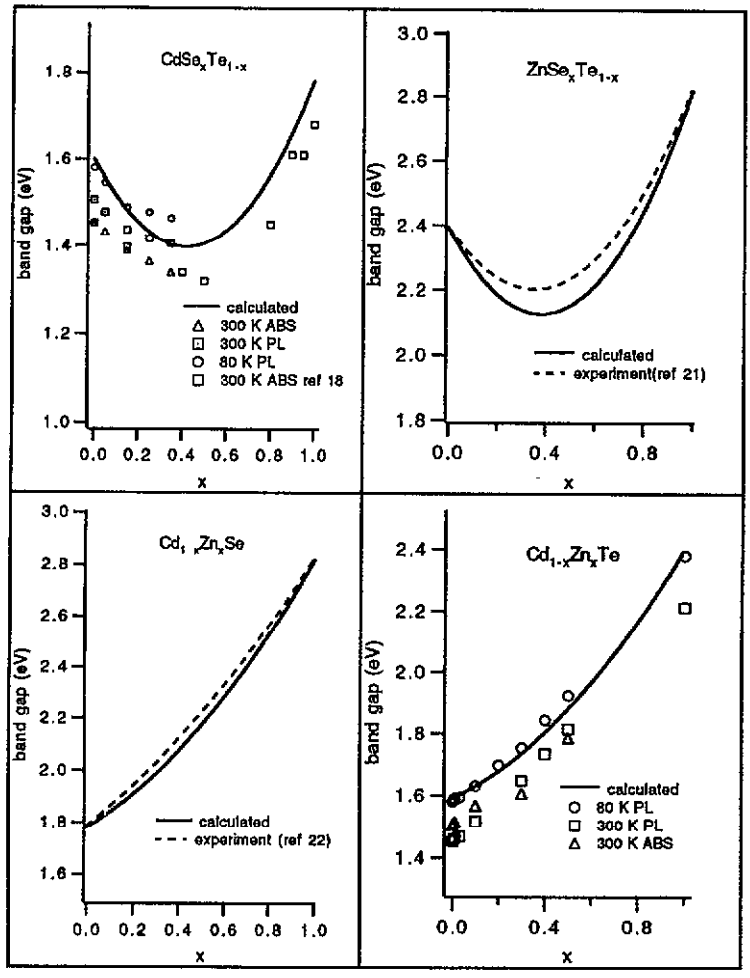

Figure 10. Calculated band gap versus composition x for II–VI ternary alloys containing Cd, Zn, Se and Te, assuming the presence of a relaxed local AuCu-I-like cluster. The calculated curve has been adjusted by an amount proportional to x so that the values at the two endpoint coincide with experimental values. Experimental data are also shown.

Comparing the values of the two structures and the experimental bowing factor, the AuCu-I-like structure in the alloy is by far the more dominant structure in $CdSe_{0.5}Te_{0.5}$.

4.3. Band structure

Taking into account both the relaxation and spin–orbit effect, the band structures of the family of alloys considered here for $x = 0.5$ are shown in figure 11. From figure 1, the local cluster has a volume twice that of the zincblende unit cell used in VCA. Therefore the band structure of the former may be considered as the folding of that of the latter (figure 5) into the first Brillouin zone of the local cluster. Most of the features in figure 11 are due to folding. As an illustration, we show in figure 12 the evolution of band structure from VCA to local cluster without relaxation for $CdSe_{0.5}Te_{0.5}$ and $Cd_{0.5}Zn_{0.5}Te$. In the VCA calculation, the pseudopotential is constructed via equation (4) as before. However, the Brillouin zone

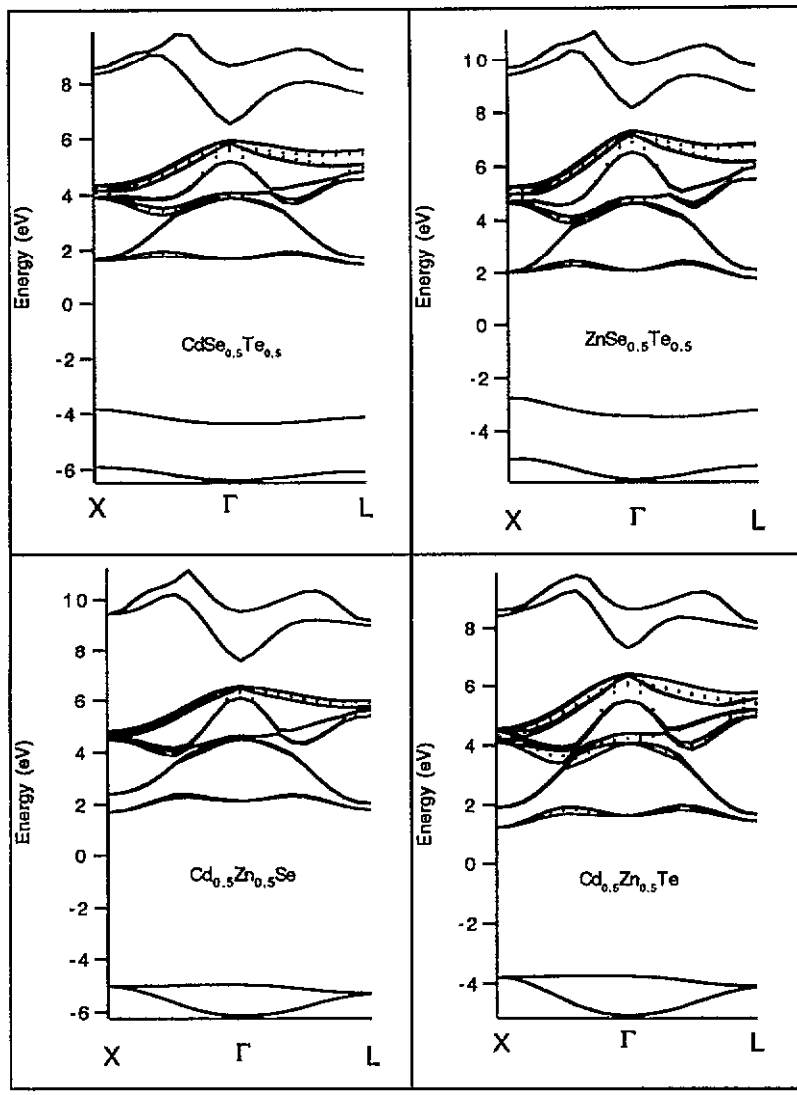

Figure 11. Calculated band structure along ΓX and ΓL for ternary II–VI semiconductor alloys containing Cd, Zn, Se and Te for $x = 0.5$, with relaxation and spin–orbit correction. (Full and dotted curves represent band structure with and without spin–orbit correction respectively.)

for AuCu-I structure is two times smaller. For the AuCu-I structure, the band structure is calculated using the Brillouin zone for the AuCu-I cell. But the band structure is extended beyond the zone boundary from Γ to X and from Γ to L, where Γ, X and L refer to the same symmetry points as in figure 5 for the zincblende Brillouin zone. The VCA band structures in figure 12 are the same as those in figure 5. The apparent difference is due to the band folding mentioned above. Comparing the VCA and local cluster band structure in figure 12, we note that, for the common-cation alloys, the lowest valence band has been split into two. For the common-anion alloys, the lowest valence band remains essentially the same as in VCA. For common-cation alloys, extra small splittings due to the ordering effect also occur at X and L for the upper valence band. The lowest conduction band is

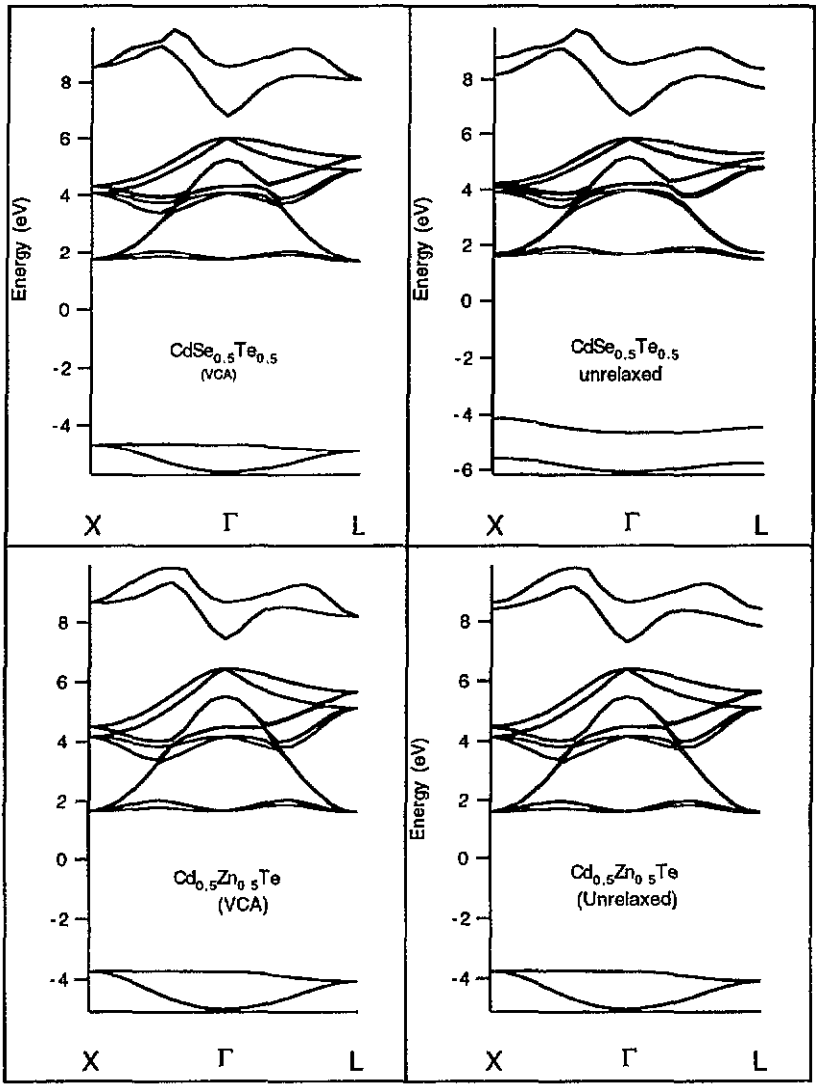

Figure 12. Calculated band structure along ΓX and ΓL for $CdSe_{0.5}Te_{0.5}$ and $Cd_{0.5}Zn_{0.5}Te$ by VCA and local cluster without relaxation. The unit cell is taken from figure 1.

also split at X and L in most cases.

When relaxation is introduced, though there exists relatively little change in the overall qualitative features, the band structure is modified quantitatively in the following three major ways:

(i) As mentioned above (see table 5), for common-cation alloys, the band gaps decrease, leading to much larger bowing factors.

(ii) For common-cation alloys, the magnitudes of the splittings are modified. This is especially pronounced for the lowest valence band and upper valence band at L. For common-anion alloys, larger splittings occur at X and L for the upper valence band.

(iii) Without relaxation, the splitting of the top valence state at Γ is very small and the state below it is singly degenerate. With relaxation, the splitting of the top valence state

at Γ is increased to about 0.11 and 0.14 eV for $CdSe_{0.5}Te_{0.5}$ and $ZnSe_{0.5}Te_{0.5}$ respectively. The corresponding splittings for the common-anion alloys are only about 0.07 eV.

Recent experimental data [28, 31] using synchrotron radiation on some of the valence band widths of CdTe and ZnTe agree quite well with our calculation [32]. Though the calculation using local density approximation underestimates the conduction band energy, it generally gives very reliable valence band energy values. With a proper implementation of disorder using local cluster with relaxation, the *ab initio* pseudopotential method can also provide us with an accurate valence band structure of II–VI alloys.

5. Conclusion

We have present a systemic study of the relativistic band structure and band-gap bowing factors of the family of semiconductor alloys containing Cd, Zn, Se and Te. As a first approximation, VCA in general explains most of the qualitative features in the band structures of the alloys. However, in order to explain the large bowing factors of the common-cation alloys, a local cluster with atomic relaxation is required in the calculation. There exists partial relaxation in the local structure of the alloys. The Zn in $ZnSe_{0.5}Te_{0.5}$ is about 78% relaxed [4] while the relaxation of Cd in $CdSe_{0.5}Te_{0.5}$ is about 67%. Under the combined effects of spin–orbit correction and structural relaxation, the relativistic band structure has been mapped out for the family of alloys considered. With relaxation, extra splittings are introduced in addition to those by spin–orbit effect. In particular, the splitting at the top of the valence band at Γ is increased. The splitting due to structural relaxation is about 0.11 and 0.14 eV for $CdSe_{0.5}Te_{0.5}$ and $ZnSe_{0.5}Te_{0.5}$ respectively.

The presence of the clusters considered theoretically is supported by the recent combined Raman and infrared spectroscopic measurements on these CdSeTe samples [19]. A third mode besides the CdTe- and CdSe-like transverse optical (TO) phonon modes in the Fourier-transform infrared (FTIR) reflectivity was suggested to arise from non-random atomic clustering. Although there are substantial amounts of experimental evidence for the existence of local order, detailed experimental mapping of the band structure of II–VI semiconductor alloys is still lacking. Comparison of band structure calculation and photoemission experiments with synchrotron radiation is expected to contribute to a more quantitative understanding of the local structure of atoms in II-VI semiconductor alloys.

Acknowledgments

We acknowledge Dr P Becla for growth of experimental samples, Professor G D Pitt and Dr K P Williams for use of the Renishaw Raman microscope, Professors S Perkowitz and S H Tang for help and support and Mr Y M Goh for technical assistance in this work.

References

[1] Van Vechten J A and Bergstresser T K 1970 *Phys. Rev.* B **1** 3351

[2] Chadi D J 1977 *Phys. Rev.* B **16** 790
Fedders P A and Myles C W 1984 *Phys. Rev.* B **29** 802

[3] Baldereschi A, Hess E, Maschke K, Neumann H, Schulze K R and Unger K 1977 *J. Phys. C: Solid State Phys.* **10** 4709
Feng Y P, Teo K L, Li M F, Poon H C, Ong C K and Xia J B 1993 *J. Appl. Phys.* **74** 3948

[4] Bernard J E and Zunger A 1987 *Phys. Rev.* B **36** 3199
Wei S H and Zunger A 1991 *Phys. Rev.* B **43** 1662
[5] Kleinman L 1980 *Phys. Rev.* B **21** 2630
[6] Bachelet G B, Hamann D R and Schluter M 1982 *Phys. Rev.* B **26** 4199
[7] Mikkelsen J C and Boyce J B 1982 *Phys. Rev. Lett.* **49** 1412
[8] Weil R, Nkum R, Muranevich E and Benguigui L 1989 *Phys. Rev. Lett.* **62** 2744
[9] Beshah K, Zamir D, Becla P, Wolff P A and Griffin R G 1987 *Phys. Rev.* B **36** 6420
[10] Kobayashi A and Roy A 1987 *Phys. Rev.* B **35** 5611
[11] Carles R, Landa G and Renucci J B 1985 *Solid State Commun.* **53** 179
[12] Spicer W E, Silberman J A, Morgan J, Lindau I, Wilson J A, Chen A B and Sher A 1982 *Phys. Rev. Lett.* **49** 948
[13] Tsang K L, Rowe J E, Callcott T A and Logan R A 1988 *Phys. Rev.* B **38** 13277
[14] Wei S H and Zunger A 1988 *Phys. Rev.* B **37** 8958
[15] Surh M P, Li M F and Louie S G 1991 *Phys. Rev.* B **43** 4286
[16] Ceperly D M and Alder B J 1980 *Phys. Rev. Lett.* **45** 566
[17] Godby R W, Schluter M and Sham L J 1987 *Phys. Rev.* B **36** 6497
[18] Perkowitz S, Kim L S, Feng Z C and Becla P 1990 *Phys. Rev.* B **42** 1455
[19] Feng Z C, Becla P, Kim L S, Perkowitz S, Feng Y P, Poon H C, Williams K P and Pitt G D 1994 *J. Cryst. Growth* **138** 239
[20] Prytkina L V, Volkov V V, Mentser A N, Vanyukov A V and Kireev P S 1968 *Sov. Phys.–Semicond.* **2** 509
[21] Cohen M L and Chelikowsky J R 1988 *Electronic Structure and Optical Properties of Semiconductors* (Berlin: Springer)
[22] Brasil M J S P, Tamargo M C, Nahory R E, Gilchrist H L and Martin R J 1991 *Appl. Phys. Lett.* **59** 1206
[23] Brasil M J S P, Nahory R E, Turco-Sandroff F S, Gilchrist H L and Martin R J 1991 *Appl. Phys. Lett.* **58** 2509
[24] Areshkin A G, Pekar G S, Polisskii G N, Popova T B, Suslina L G and Fedorov D L 1986 *Sov. Phys.–Solid State* **28** 2109
[25] Shalimova K V, Botnev A F, Dmitriev V A, Kognovitskaya N Z and Starostin V V 1970 *Sov. Phys.–Crystallogr.* **14** 531
Brafman O 1972 *Solid State Commun.* **11** 447
[26] Gross E F, Suslina L G and Kon'kov P A 1962 *Sov. Phys.–Solid State* **4** 287
[27] Madelung O, Schulz M and Weiss H (ed) 1982 *Numerical Data and Functional Relationships in Science and Technology (Landolt-Borstein* New Series, vol 17b) (Berlin: Springer)
[28] Niles D W and Hochst H 1991 *Phys. Rev.* B **43** 1492
[29] Ley L, Pollak A, McFreely F R, Kowalczyk S P and Shirley D A 1974 *Phys. Rev.* B **9** 600
[30] Landau L D and Lifshitz E M 1969 *Statistical Physics* (Oxford: Pergamon)
Khachaturyan A G 1983 *Theory of Structural Transformations in Solids* (New York: Wiley)
[31] Niles D W and Hochst H 1992 *Phys. Rev.* B **46** 1498
[32] Poon H C, Feng Y P, Ong C K and Li M F unpublished